



## POST-TENSIONING LOSS INFLUENCE ON THE SEIMIC RESPONSE OF TIMBER FRAMES

G. Granello <sup>(1)</sup>, T. Smith <sup>(2)</sup>, F. Sarti <sup>(3)</sup>, D. Moroder <sup>(4)</sup>, A. Palermo <sup>(5)</sup>, S. Pampanin <sup>(6)</sup>

<sup>(1)</sup> PhD Candidate, University of Canterbury, gabriele.granello@pg.canterbury.ac.nz

<sup>(2)</sup> Structural Timber Research Engineer, University of Canterbury, tobias.smith@canterbury.ac.nz

<sup>(3)</sup> Structural Timber Research Engineer, University of Canterbury, francesco.sarti@canterbury.ac.nz

<sup>(4)</sup> Structural Timber Research Engineer, University of Canterbury, daniel.moroder@canterbury.ac.nz

<sup>(5)</sup> Associate Professor, University of Canterbury, alessandro.palermo@canterbury.ac.nz

<sup>(6)</sup> Professor, University of Canterbury, stefano.pampanin@canterbury.ac.nz

### **Abstract**

As a result of the Precast Seismic Structural System (PRESS) program in the 1990s coordinated by the University of California, San Diego, the hybrid connection proved to be an efficient solution for achieving low damage concrete buildings. The combination of unbonded post-tensioning tendons and mild steel bars, allows the accommodation of the seismic demand through controlled rocking between structural members. While tendons provide the system re-centering capability after a seismic event, dissipation is localized to specific replaceable elements.

In 2005 the technology was extended to engineered wood materials such as Laminated Veneer Lumber (LVL), glue laminated timber and cross laminated timber. Extensive laboratory tests carried out at the University of Canterbury showed good results in the connection performance, with no residual damage in the remaining structure. However, there is still little information about the long term behavior of post-tensioned timber, related in particular to the amount of possible post-tensioning loss due to creep effects arising inside compressed members. The beam-column joint detailing represents in fact a critical part in terms of creep development, since timber column is loaded perpendicular to the grain.

A case study building is presented in this paper, where the expected amount of post-tensioning loss varies between 5% and 45% in 50 years depending on the joint detailing solution. Two possible alternatives in the column-foundation connection are proposed, assuming different non-structural components drift resilience. The building seismic response is then analysed for different scenarios of post-tensioning loss up to 90% of the initial value. For this, Acceleration-Displacement Response Spectra (ADRS) and Non Linear Time History Analysis (NLTH) are applied and compared to investigate the structural behaviour considering events with return period equal to 50 years (SLS) and 500 years (ULS).

The numerical results are then presented and discussed in terms of drift, accelerations, damping, and residual deformations. The seismic response in terms of re-centering capacity, drift control and dissipation properties is found satisfactory for post-tensioning loss up to 50%. In case of greater amount of loss (i.e. 90%) the seismic behaviour is still acceptable providing however a residual drift.

*Keywords: Post-tensioned timber; Post-tensioning loss; Rocking connection;*

## 1. Introduction

Pres-Lam (Prestressed Laminated Timber) technology takes advantage of unbonded post-tensioned steel tendons or bars passing through internal ducts in timber beams, frames or walls, to create moment resisting connections [1]. The principles behind the technology are based on the PRESSSS-hybrid connections developed by Priestley [2,3] and Pampanin [4]. The system accommodates the seismic demand through controlled rocking between structural elements and tendon elongation, which provides re-centering capability. Energy dissipation is obtained by introducing replaceable mild steel bars or other types of energy release devices generally called “dissipaters”. In 2002 Christopoulos et al. [5] extended the concept to steel members, proving the technology being material independent. In 2005 the so called “hybrid rocking connection” was extended to engineered timber products by Palermo et al. [6, 7].

Extensive laboratory tests conducted at the University of Canterbury [8-10] showed the good seismic performance of the connection in timber structures, with no residual damage in the structural members. Numerical models were developed to capture the behaviour of post-tensioned timber walls [11] and post-tensioned timber frames [12-13], with very satisfactory results in terms of accuracy. A detailed design procedure was also proposed for this type of buildings [1].

Even if Pres-Lam is currently being researched and implemented all over the world with many buildings in New Zealand in the last decade (see Figure 1) [14,15], further research on the long term performance of this technology needs to be performed in order to optimize the current design.



Figure 1: Trimble Office, Christchurch: a) aerial view and d) post-tensioning operations, Merritt building, Christchurch: b) aerial view. Massey University, Wellington: c) aerial view. (Images courtesy of Andy Buchanan, with permission).

The influence of post-tensioning loss deriving from creep phenomena in compressed timber members can affect the whole structural behaviour. The possible amount of loss is estimated to reach values between 6-50% in most practical cases, mainly depending on the quantity of timber loaded perpendicular to grain [16, 17]. For this reason, frame structures are more likely than walls to sustain post-tensioning loss, which requires more attention when the beam-column joints.

Different design solutions have been implemented in real buildings to avoid loading timber perpendicular to the grain, such as the employment of steel plates or rotated timber panels. The use of steel plates in columns as designed for the Trimble Office in Christchurch (Figure 2a) proved to be a possible solution to control the post-tensioning loss. The structure is being monitored and the amount of loss in 4 different locations is in between 2% and 8% in 2 years.

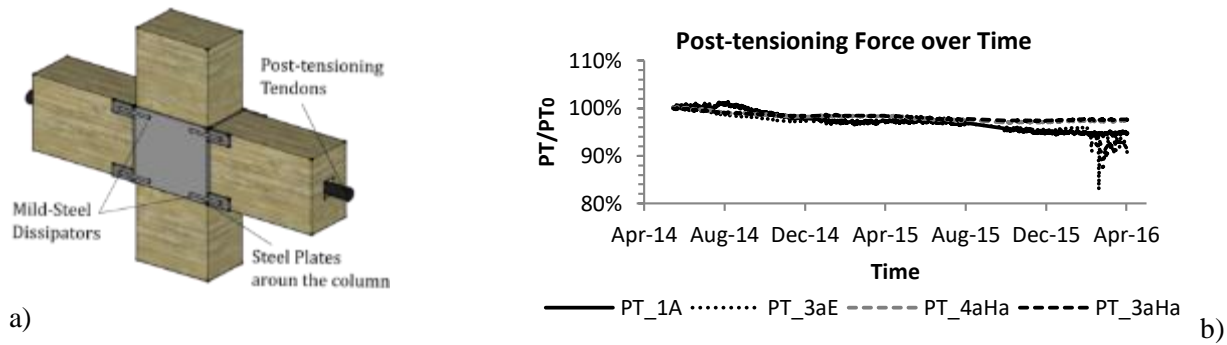


Figure 2: Post-tensioning force over time for Trimble Office, Christchurch: a) joint detailing and b) post-tensioning under monitoring in 4 beam-column joints.

In this paper, the structural performance of a case study building with post-tensioned LVL timber frames is investigated considering different scenarios in terms of post-tensioning loss, column-foundation connection and different return period events. In particular, the results obtained by Non Linear Static Analyses (Pushover), Acceleration-Displacement Response Spectra (ADRS) and Non Linear Time History Analyses (NLTH) will be presented and discussed.

## 2. Building Design

In order to investigate the influence of post-tensioning loss on the seismic behaviour of Pres-Lam frame structures, a case study building is proposed and analysed. The building presents 4 suspended floors with a lightweight timber penthouse on top of the fourth floor (Figure 3). The building is 32×19.5m in plan with a total floor area of 624 m<sup>2</sup>. The building is designed to be located in Christchurch on a soil type D (soft or deep soil) condition according to the New Zealand Standard [18]. The lateral load resistance is provided by post-tensioned moment frames in the transverse direction and post-tensioned walls in the longitudinal direction.

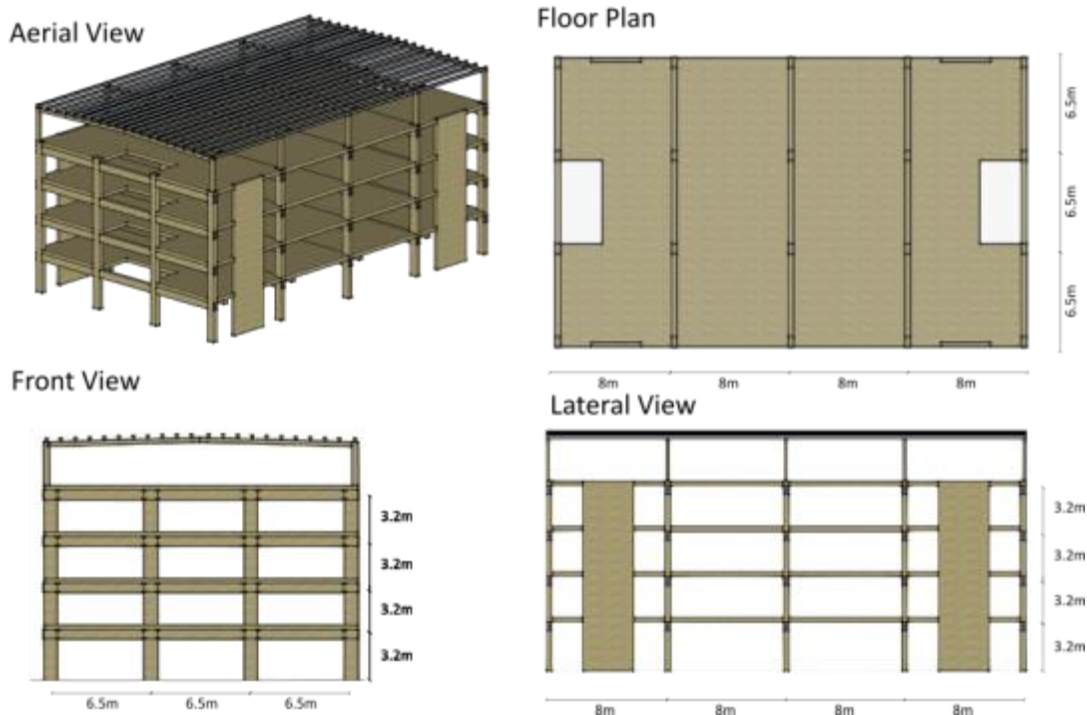


Figure 3: Case study building.

The floor system is made up of 21mm thick plywood panels on top of 90x400 mm timber joist (Figure 4). Considering a live load equal to 3kPa (office use in accordance to the New Zealand Standard [18]) the seismic weights are as reported in Table 1.

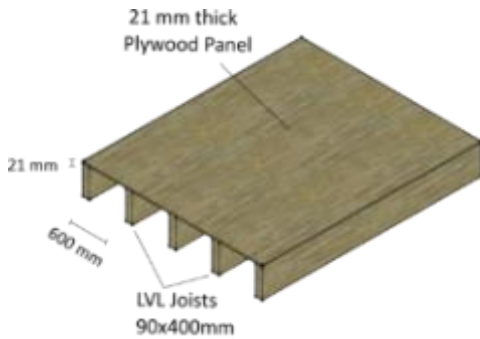


Figure 4: Timber floor.

Table 1: Structural Seismic masses.

Seismic masses			
Floor	[KN]	[KN]/frame	[KN]/wall
4	3130	626	782
3	3193	639	798
2	3193	639	798
1	3193	639	798
<b>Tot</b>	<b>12710</b>	<b>2542</b>	<b>2542</b>

A 1/500 years return period event ( $Z=0.3$ ) is considered for the Ultimate Limit State (ULS) and a 1/50 years return period event ( $Z=0.86$ ) is considered for the Service Limit State (SLS). In terms of beam-column joint two possible solutions are proposed (Figure 5):

- a) A beam-panel (BP) rocking connection
- b) A beam-column (BC) rocking connection

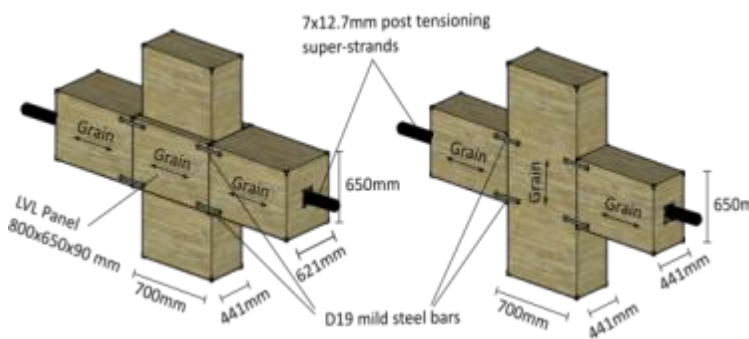


Figure 5 Different joint solutions: beam-panel (BP) and beam-column (BC).

Table 2: Post-tensioning loss for different beam-column joint solution and different relative humidity (RH) conditions.

Years	40% < RH < 50%		40% < RH < 90%	
	BP	BC	BP	BC
1	1.5%	5.1%	1.8%	5.4%
5	2.3%	11.8%	3.0%	12.7%
10	3.1%	19.6%	4.1%	21.2%
20	3.9%	28.2%	4.9%	30.3%
50	5.3%	42.9%	5.9%	44.8%

The reason for a different detailing is related to the long term behaviour of timber in terms of creep effects which influences the amount of post-tensioning loss. The analytical model developed by Fragiaco and Davies [17] was used to evaluate the amount of post-tensioning loss. To estimate the timber moisture content in order to assess the mechano-sorptive creep, a diffusion analysis over the LVL sections was carried out [19] considering low relative humidity (RH) annual cycles (40% < RH < 50%) and high relative humidity (RH) annual cycles (40% < RH < 90%). Results in terms of post-tensioning loss are reported in Table 2.

The design of the building was carried out setting the performance at the SLS. Two levels of drift limits were defined as design goals:

- 1) 0.5%, which is suitable for common non-structural brittle elements (panels, windows, glasses);
- 2) 1%, which is suitable in case of low damage non-structural elements [20], [21];

This drift limits can be achieved by using one of the two column-foundation connection as shown in Figure 6 without changing the geometry and reinforcement layout of the beam-column joint. A pin-base connection, quite common in most timber structures, would increase the inter-storey drift compared to a more rigid connection. Conversely, a semi-rigid moment-resisting connection with epoxied bars would limit the drift, but the bars

would be subjected to plastic deformation for seismic demands exceeding a design threshold. This last solution can be also realized by using external dissipaters. The designer can therefore decide which elements will be subjected to damage depending on the event probability, and based on the initial/repairing cost find the optimum solution case by case. Displacement Based Design method [22] was used to check the displacements at the ULS against a maximum allowable drift limit equal to 2% .

In this case study, the semi-rigid column-foundation connection was designed with internal bars to yield only for events with annual probability greater than 1/50. An embedment length of 500 mm was necessary to avoid pulling-out failures of the bars and an unbonded length of 200 mm was selected to confine the steel deformation within 4 %.

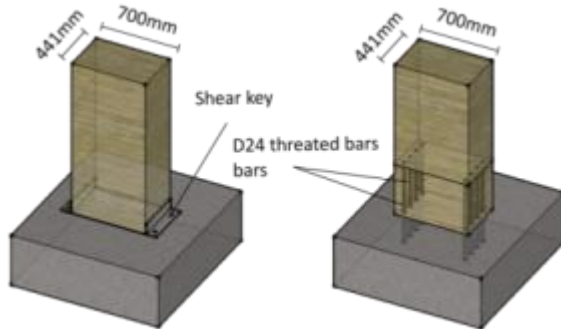


Figure 6: Pin-base connection and semi-rigid connection.

The hybrid rocking connection was designed considering a re-centering ratio,  $\beta$ , (defined as the ratio between the moment due to post-tensioning over the total connection moment capacity) of 0,6 . 7-wire strands were used for the post-tensioning, while dissipation was provided through mild steel bars. As reported in Table 3, two different layouts with varying number of tendons and amount of dissipaters were used for the connections at the two bottom and the two top storeys, respectively.

### 3.1 Push-pull Static Analysis: Connection Behaviour

Depending on the joint detailing and on the humidity cycles the structure is subjected to, the amount of post tensioning loss at 50 years is estimated to be between 5% and 45% of the initial value (Table 2). The moment-rotation behaviour of the connections was evaluated using an iterative procedure [23] and implemented in a finite element model (see Figure 7) by a combination of rigid links and rotational springs. In particular two rotational springs combined in series were used: one multi-elastic describing the post-tensioning contribute and one elasto-plastic with strain hardening describing the mild steel contribute. The results are shown in Figure 8.

Different post-tensioning losses ranging from 0 to 90% were considered. The post-tensioning loss has three main effects as shown in Figure 8. The first one is the decrease of the decompression moment, which is defined as the moment value at 0 interface rotation. As the decompression moment depends on the axial forces acting on the section, the gap opening is activated earlier as the post-tensioning force drops. The second effect is the connection maximum capacity. As the contribution given by post-tensioning is reduced, the total capacity being the sum of post-tensioning and mild steel is also reduced. The third effect is the increasing residual rotation which is the result of the loss in re-centering capacity.

Although these general considerations were drawn from static cyclic analysis of the single connection, further analysis were deemed necessary to provide an exhaustive discussion on the influence of post-tensioning loss on the system behaviour. These outcomes are discussed later in Section 3.2 and Section 3.3.

Table 3: Force level and dissipaters detailing in the hybrid connections.

Storey	Tendons number	Tendons Stress [% $f_{p01k}$ ]	Mild Steel Bars
1&2	7	64%	4 $\phi$ 19
3&4	5	64%	4 $\phi$ 16

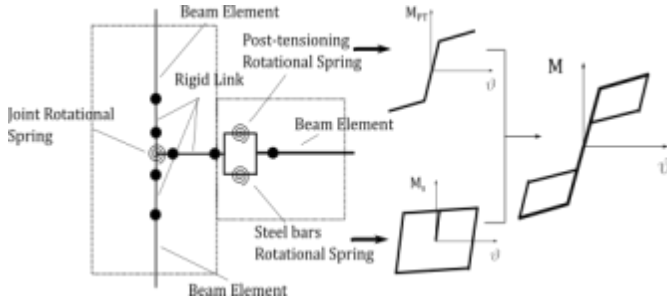


Figure 7: Hybrid connection modelling.

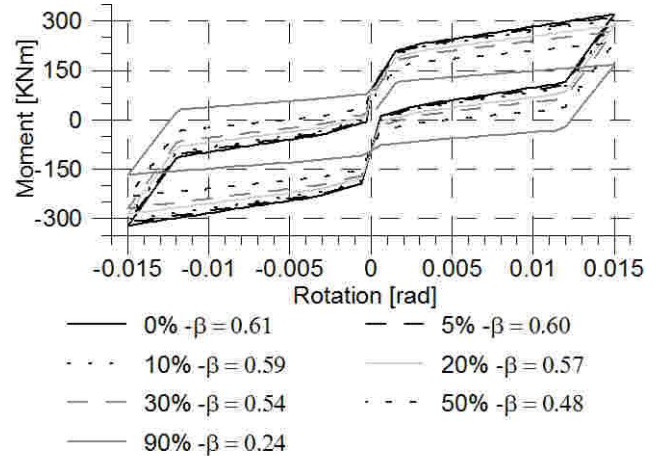


Figure 8: Moment rotation behaviour for different levels of post-tensioning loss from 0 to 90%.

### 3.2 Static Analysis: Building Behaviour

The Acceleration-Displacement Response Spectrum analysis [24] was carried out in order to evaluate the global building performance at the SLS and at the ULS. In Figure 9a) the response of the case building designed with semi-rigid connection is presented. The results for the pin-base building are similar and not reported for space requirements.

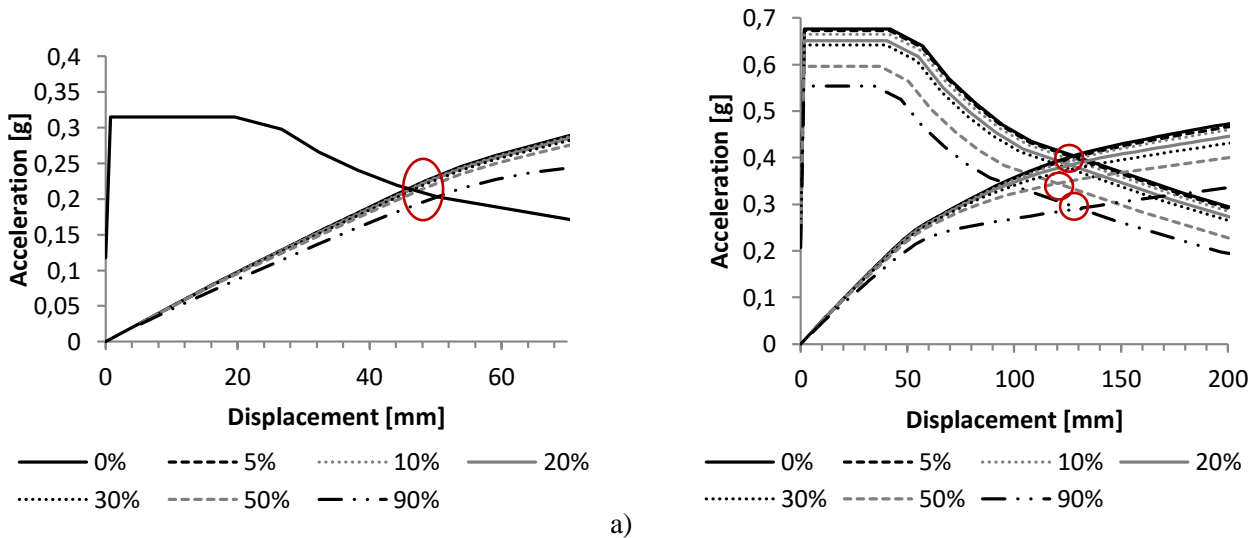


Figure 9: ADRS Spectra considering the semi-rigid base connection: a) SLS and b) ULS

It can be noticed that the influence of post-tensioning losses on the building performance at the SLS is negligible up to a 50% loss. This was an expected outcome as the SLS moment demand on the beam-column joint does not exceed the decreased decompression moment, i.e. no gap opening in the joint but mainly elastic deformation.

A more interesting change in behaviour was observed at ULS. The plots in Figure 9b show that the decrease in post-tensioning force does not significantly affect the displacement demand of the structure which remains within 120 and 130 mm, i.e. drift 1%. This is due to both the damping  $\xi$  and the ductility  $\mu$  of the system increasing for higher levels of post-tensioning loss as reported in Table 4. Since the lower level of post-tensioning force, the connection opens earlier the gap and the steel is earlier activated starting dissipating energy at lower level of drift. As a result, ductility and damping are increased. At the same time, the strain in the

dissipaters  $\epsilon_{diss}$  increases due to the anticipate gap opening for equal levels of drift as reported in Table 4. The strain in the dissipater is reported as ratio over the rupture limit  $\epsilon_u$  assumed equal to 6%. The connection hysteretic damping  $\xi_{hyst,conn}$  is defined [25] as:

$$\xi_{hyst,conn} = \frac{A_{diss}}{2\pi\Delta_s F_s}; \quad \text{Equation 1}$$

where  $A_{diss}$  represents the area enclosed in one complete cycle of a stabilized force-displacement loop (or moment-rotation) diagram;  $\Delta_s$  and  $F_s$  are the maximum peak displacement and peak force, respectively.

As shown in Figure 8, the area enclosed in the moment-rotation loop remains constant regardless the post-tensioning loss. Conversely, the peak force decreases with increasing post-tensioning loss. Therefore, according to Equation 1, post-tensioning loss causes both a reduction of stiffness and a greater damping at connection level, which at the building level produces similar displacements. At building level, the hysteretic damping  $\xi_{hyst,str}$  can be expressed based on the same principle as in Equation 1[1]:

$$\xi_{hyst,str} = \frac{(2-2\beta)(\mu-1)}{\mu\pi(1+r(\mu-1))} \quad \text{Equation 2}$$

where  $\mu$  represents the structural ductility,  $\beta$  the global re-centering ratio and  $r$  the post-yield stiffness ratio. The total structural damping  $\xi$  is a combination between hysteretic damping, ductility and elastic damping [1]:

$$\xi = \mu^{-0.43}\xi_{el} + 0.65\xi_{hyst,str} \quad \text{Equation 3}$$

In Figure 10 the total damping is plotted against the post-tensioning loss. It can be noticed that the damping value increases from 9-11% with initial post-tensioning to 17-20% in case of post-tensioning loss equal to 90%.

Table 4: Ductility  $\mu$ , damping  $\xi$ , drift and dissipation strain  $\epsilon_{diss}$  over the ultimate strain  $\epsilon_u$  for different levels of post-tensioning loss.

	PT Loss	$\mu$	$\xi$	Drift	$\epsilon_{diss}/\epsilon_u$
<b>Semi-rigid</b>	0%	1.6	10.7%	1.22%	13%
	20%	1.68	11.6%	1.22%	13%
	50%	1.8	13.6%	1.22%	14%
	90%	2	17.4%	1.21%	16%
<b>Pin</b>	0%	1.55	9.4%	2.00%	42%
	20%	1.75	10.9%	2.00%	44%
	50%	2	13.9%	1.85%	45%
	90%	2.3	19.8%	1.70%	50%

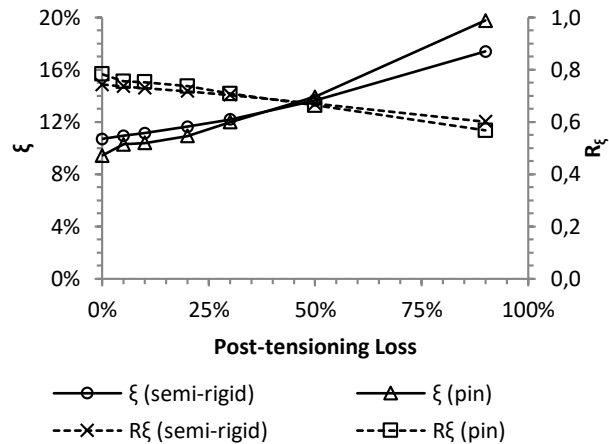


Figure 10: Damping  $\xi$  and Spectral Reduction Factor  $R_\xi$  for different amounts of post-tensioning loss.

On the right vertical axis of Figure 10, the damping-proportional spectral reduction factor  $R_\xi$  [18] is also plotted for different levels of post-tensioning loss. The spectral reduction factor decreases from 0.75 at the initial state, to 0.6 corresponding to 90% of post-tensioning loss.

### 3.3 Dynamic Analysis: Building Behaviour:

To further investigate the building performance a Non Linear Time History Analysis was performed. The ground motion selection and scaling process was carried out according to the New Zealand Standards [18]. The building period was estimated to be 0.85 s for the semi-rigid connection and 1.2 for the pinned connection. The ground

motions were selected from the NGA database [26] and are reported in Table 5. Their average spectra after the scaling process is shown in Figure 11 and compared with the ULS code target spectrum[18].

In the first stage of the dynamic analyses, the case study buildings were subjected to SLS intensity earthquakes with the drift and column moments envelope results shown in Figure 12 .

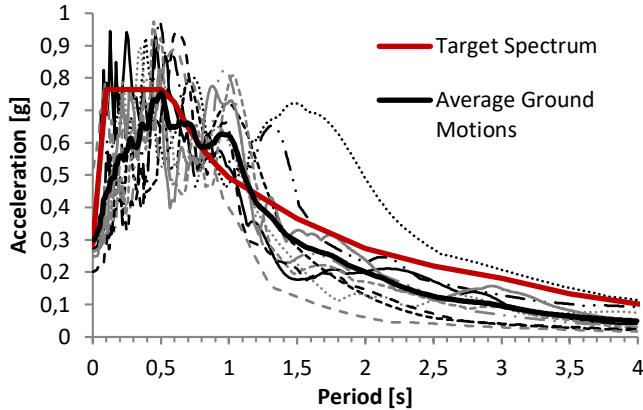
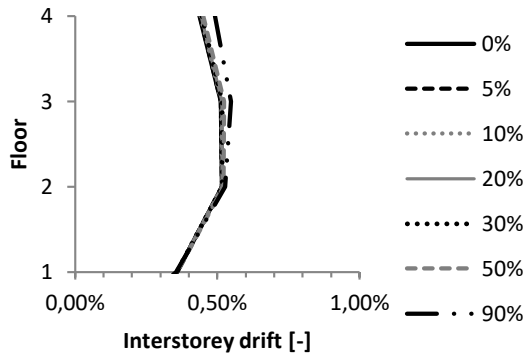


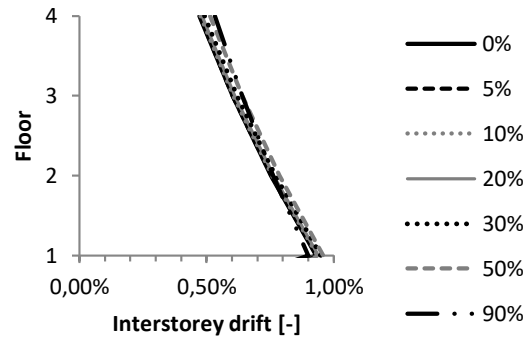
Figure 11: Ground motions spectra.

Table 5: Selected ground motions from the NGA Database.

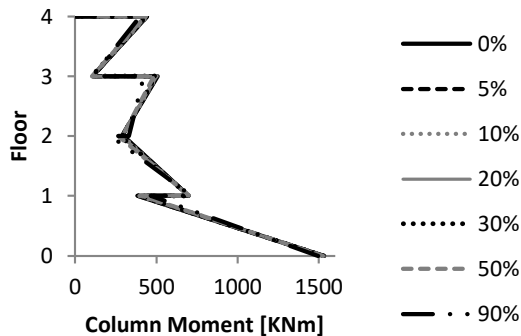
Sequence Number	Earthquake Name	YEAR
6	Imperial Valley-02	1940
20	Northern Calif-03	1954
70	San Fernando	1971
170	Imperial Valley-06	1979
289	Irpinia, Italy-01	1980
322	Coalinga-01	1983
339	Coalinga-01	1983
359	Coalinga-01	1983
363	Coalinga-01	1983
415	Coalinga-05	1983



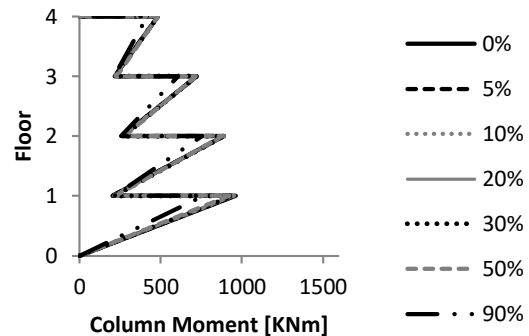
a)



b)



c)



d)

Figure 12: Drift profile at the SLS: a) semi-rigid base connected building and b) pin base connected building for different levels of post-tensioning loss. Column-moment profile at the SLS: c) semi-rigid base connected building and d) pin base connected building for different levels of post-tensioning loss.

The drift profiles in Figure 12a and b show that the post-tensioning loss does not significantly affect the maximum displacements, confirming the observations of Section 3.2. The drift profiles reveal that the critical

floors are at the middle storeys for the fully-fixed base connection and at the 1<sup>st</sup> storey for the pin base connection. Furthermore, the pin connection introduces more flexibility in the building which increases the maximum drift (1% against 0.5%). The influence of the base connection can be also noticed on the columns moment distribution. The maximum value between the columns is reported in Figure 12c and d. The fully-fixed base connection in fact attracts the seismic force at the base, whereas the pin connection spreads the demand among the different joints up the building height.

The NLTHA results at ULS are reported in Figure 13. Similarly to the ADRS results (see Section 3.2), the difference in terms of drift is small in both the semi-rigid and pin base connected cases. A slightly greater difference is noticeable for the pin-base case; this is due to building capacity totally relying on the beam-column connection contribution. Conversely, the semi-rigid case relies on both the beam-column connections and moment base connections.

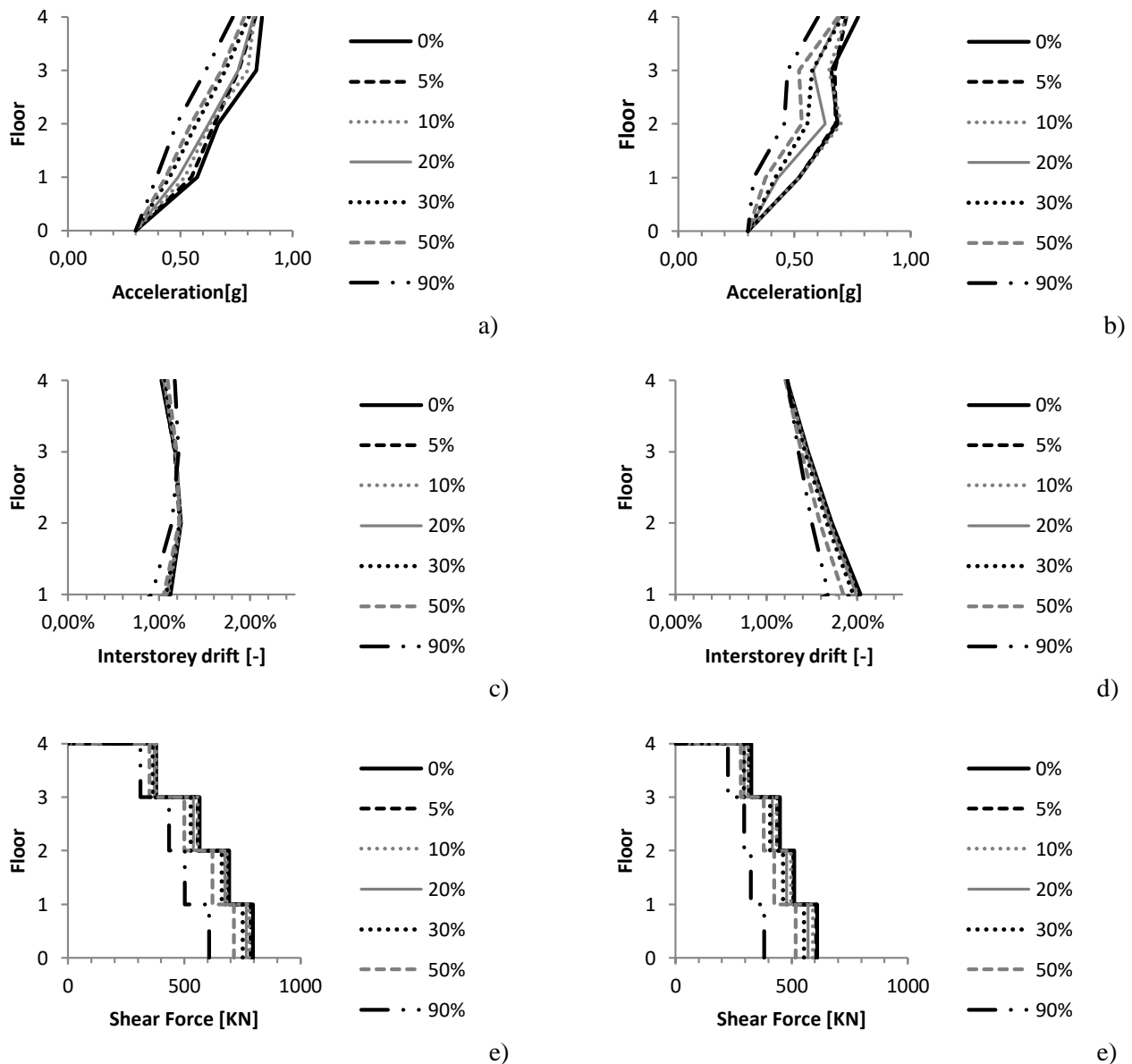


Figure 13: Acceleration profile at the ULS: a) semi-rigid base connected building and b) pin base connected building. Drift profile at the ULS: c) semi-rigid base connected building and d) pin base connected building.

Base shear profile at the ULS: e) semi-rigid base connected building and f) pin base connected building. All the results are expressed for different levels of post-tensioning loss.

In terms of floor shear demand distribution and floor accelerations, a decreasing value can be noticed for greater level of post-tensioning loss. These results are consistent with the ADRS response: while the displacements remain similar, the accelerations are reduced with increasing post-tensioning loss. This is again due to the increased amount of damping caused by the decreased post-tensioning contribution.

In Figure 14 the top floor displacement due to the 6<sup>th</sup> ground motion is presented for the semi-rigid case considering 0% and 90% of post-tensioning loss. It can be noticed the greater residual displacement due to greater post-tensioning loss as the structure loses part of its re-centering capacity. The global re-centering capacity can be calculated averaging the re-centering ratio of every connection weighed on the moment contribution with respect to the global over-turning moment induced by the earthquake [1]. This value is plotted in Figure 15 against the post-tensioning loss.

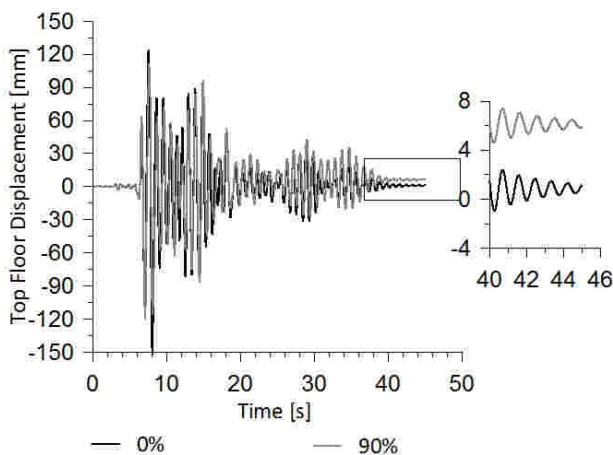


Figure 14: Top floor displacement for 0% and 90% values of post-tensioning loss due to the 6<sup>th</sup> ground motion in the semi-rigid case.

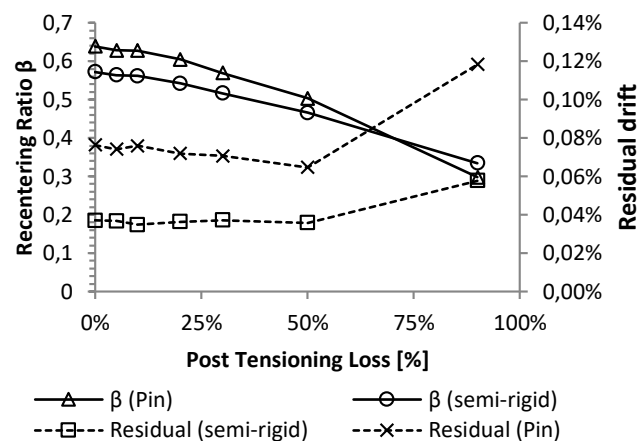


Figure 15: Re-centering ratio and residual drift depending on the post-tensioning loss.

It can be noticed that the global re-centering ratio decreases with decreasing force in the tendons; this effect is more pronounced for the semi-rigid case. As the semi-rigid connection has a moment contribution at the base with low re-centering ratio (around 0.3 due to gravity loads), the overall value of  $\beta$  is lower than for the pin case, where the moment contribution depends only on the hybrid connections.

In terms of maximum residual drift as shown in Figure 15, it can be seen that the building's re-centring ability is almost unaffected for post-tensioning losses smaller than 50%. For higher losses, the hybrid connections remain in their deformed configuration as can be seen in Figure 8 and the building suffers higher residual drifts.

#### 4. Conclusion

This paper presents an extensive numerical study aimed to assess the influence of post-tensioning loss on the seismic behaviour of Pres-Lam frames.

The amount of post-tensioning loss expected in a well-designed post-tensioned LVL timber frame can vary between 5% and 45% in 50 years depending on beam-to-column connection detailing and environmental conditions.

However, the SLS seismic performance of the building is independent from the post-tensioning since the structural behaviour is mainly governed by the elastic properties of the system with no gap openings in the beams.

The change in post-tensioning force influences the building re-centering and damping capabilities of the case study buildings at ULS, but the displacement demand is not significantly affected. The decreasing post-tensioning implies lower connection secant stiffness, earlier gap opening, higher damping and lower re-centering capability. Considering a real case scenario with post-tensioning loss up to 50% in 50 years, the re-centering ratio will still be maintained greater than 0.5 ensuring low levels of residual drift (below 4% of maximum peak drift).

Even in exceptional cases assuming a post-tensioning loss equal to 90%, the system's displacements do not increase excessively at the ULS although residual drifts reach values close to 12% of maximum peak drift. This is due to the damping capability of the dissipaters, which increases for lower values of post-tensioning forces.

Due to the system intrinsic robustness, which comprises of two different reinforcing elements (post-tensioning and dissipaters) PRES-LAM timber frames can achieve satisfactory low-damage performance over time despite post-tensioning loss, however MCE and collapse limit state might be compromised due to excessive strain in the dissipaters and more research needs to be carried out.

## 5. Acknowledgements

The authors also acknowledge the financial support from the Structural Timber Innovation Company (STIC).

## 6. References

- [1] S. Pampanin, A. Palermo, and A. Buchanan, *Post-Tensioned Timber buildings - Design Guide Australia and New Zealand*. Structural Timber Innovation Company, 2013.
- [2] N. M. J. Priestley, "Overview of the PRESSS Research Program," *PCI Journal*., 1991.
- [3] N. M. J. Priestley, "The PRESS program - Current status and proposed plans for phase III," *PCI Journal*, 1996.
- [4] S. Pampanin, "Emerging Solutions for High Seismic Performance of Precast/Prestressed Concrete Buildings," *Journal of Advanced Concrete Technology*, vol. 3, no. 2, pp. 207–223, 2005.
- [5] C. Christopoulos, A. Filiatrault, C. Uang, and B. Folz, "Post-Tensioned Energy Dissipating Connections for Moment Resisting Steel Frames," *Journal of Structural Engineering*, 2002.
- [6] A. Palermo, S. Pampanin, A. Buchanan, and M. Newcombe, "Seismic design of multi-storey buildings using laminated veneer lumber (LVL)," *New Zealand Society for Earthquake Engineering Conference*, Taupo, New Zealand, 2005.
- [7] A. Palermo, S. Pampanin, M. Fragiocomo, A. H. Buchanan, and B. L. Deam, "Innovative Seismic Solutions for Multi-Storey LVL Timber Buildings Overview of the research program," *World Conference on Timber Engineering*, Portland, Oregon, U.S., 2006.
- [8] M. P. Newcombe, S. Pampanin, and A. H. Buchanan, "Experimental Testing of a Two-Storey Post-Tensioned Timber Building," *Canadian Conference on Earthquake Engineering*, Toronto, Ontario, Canada, 2010.
- [9] T. Smith, S. Pampanin, D. Carradine, A. Buchanan, F. C. Ponzo, A. Di Cesare, and D. Nigro, "Experimental investigations into post-tensioned timber frames with advanced damping systems," *Italian National Association for Earthquake Engineering Conference*, Bari, Italy, 2011.
- [10] F. Sarti, A. Palermo, and S. Pampanin, "Quasi static cyclic tests of 2 / 3 scale post-tensioned timber wall and column-wall-column ( CWC ) systems," *New Zealand Society for Earthquake Engineering Conference*, Auckland, New Zealand, 2014.
- [11] F. Sarti, "Seismic Design of Low - Damage Post - Tensioned Timber Wall Systems," PhD Thesis, University of Canterbury, 2015.

- [12] A. Di Cesare, F. C. Ponzo, M. Simonetti, T. Smith, and S. Pampanin, “Numerical modeling of a post-tensioned timber frame building with hysteretic energy dissipation,” *International Conference on Structural Engineering Mechanics and Computation*, Cape Town, South Africa, 2013.
- [13] T. Smith, “Post-tensioned Timber Frames with Supplemental Damping Devices,” PhD Thesis, University of Canterbury, 2014.
- [14] C. P. Devereux, T. J. Holden, A. Buchanan, and S. Pampanin, “NMIT Arts & Media Building - Damage Mitigation Using Post-tensioned Timber Walls,” *Pacific Conference on Earthquake Engineering*, Auckland, New Zealand, 2011.
- [15] B. Curtain, D. Dekker, S. . . Chung, and A. Palermo, “Design of Carterton Event Centre: an example of innovative collaboration between architecture and timber engineering,” *World Conference on Timber Engineering*, Auckland, New Zealand, 2012.
- [16] M. Davies and M. Fragiacomio, “Long-Term Behavior of Prestressed LVL Members. I: Experimental Tests,” *Journal of Structural Engineering*, vol. 137, no. 12, pp. 1553–1561, 2011.
- [17] M. Fragiacomio and M. Davies, “Long-Term Behavior of Prestressed LVL Members. II: Analytical Approach,” *Journal of Structural Engineering*, vol. 137, no. 12, pp. 1562–1572, 2011.
- [18] Standards New Zealand, *NZS 1170.5: Structural Design Actions- Earthquake Actions*. 2004.
- [19] G. Granello, S. Giorgini, A. Palermo, and S. Pampanin, “Post-Tensioned LVL Beams : Experimental Results and Numerical Modelling,” *World Conference on Timber Engineering*, Vienna, Austria, 2016.
- [20] A. Baird, A. Palermo, S. Pampanin, P. Riccio, and A. S. Tasligedik, “Focusing on reducing the earthquake damage to facade systems,” *Bulletin of New Zealand Society for Earthquake Engineering* vol. 44, no. 2, 2011.
- [21] A. S. Tasligedik, “Damage Mitigation Strategies for Non-Structural Infill Walls,” PhD Thesis, University of Canterbury, 2014.
- [22] N. M. J. Priestley, G. M. Calvi, and M. J. Kowalsky, *Displacement-Based Seismic Design of Structures*, IUSS Press, 2007 .
- [23] M. P. Newcombe, S. Pampanin, A. Buchanan, and A. Palermo, “Section Analysis and Cyclic Behavior of Post-Tensioned Jointed Ductile Connections for Multi-Story Timber Buildings,” *Journal of Earthquake Engineering*, vol. 12, no. sup1, pp. 83–110, 2008.
- [24] A. K. Chopra and K. G. Rakesh, “Capacity-Demand-Diagram Methods based on Inelastic Design Spectrum,” *Earthquake Spectra*, vol. 4, no. 15, 1999.
- [25] L. S. Jacobsen, “Damping in composite structures,” *World Conference on Earthquake Engineering*, Tokyo and Kyoto, Japan, 1960.
- [26] B. Chiou, R. Darragh, N. Gregor, and W. Silva, “NGA project strong-motion database,” *Earthquake Spectra*, vol. 24, no. 1. pp. 23–44, 2008.